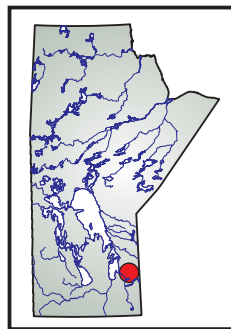


The Mayville mafic–ultramafic intrusion in the Neoarchean Bird River greenstone belt, southeastern Manitoba (part of NTS 52L12): preliminary geochemical investigation and implication for PGE-Ni-Cu-(Cr) mineralization

by X.M. Yang, H.P. Gilbert, M.T. Corkery and M.G. Houle¹

Yang, X.M., Gilbert, H.P., Corkery, M.T. and Houle, M.G. 2011: The Mayville mafic–ultramafic intrusion in the Neoarchean Bird River greenstone belt, southeastern Manitoba (part of NTS 52L12): preliminary geochemical investigation and implication for PGE-Ni-Cu-(Cr) mineralization; *in Report of Activities 2011*, Manitoba Innovation, Energy and Mines, Manitoba Geological Survey, p. 127–142.



Summary

The Mayville mafic–ultramafic intrusion, consisting of anorthosite, leucogabbro, gabbro, melagabbro and pyroxenite, is located in the Neoarchean Bird River greenstone belt, approximately 145 km northeast of Winnipeg. The intrusion contains a significant amount of platinum group element (PGE), Cu, Ni and locally Cr minerals, as indicated by recent mineral exploration. Mustang Minerals Corp. reported that the Mayville property (M2 deposit), a part of the Mayville intrusion, has an NI 43-101 open-pit mineral resource (indicated category) consisting of 9.2 million tonnes averaging 0.61% Cu, 0.23% Ni and 0.43 g/t combined precious metals (Pd+Pt+Au). The Mayville deposit appears to be open along strike and to depth, but requires more diamond drilling and detailed geological and geochemical investigations to identify the full extent of the mineral resource, and to improve the understanding of the metallogeny of the Mayville intrusion. An exploration target such as that within the Mayville intrusion (i.e., stratabound PGE-enriched sulphide- and chromite-bearing layers), although attractive, is difficult to delineate. Questions that need to be addressed include the following:

- What are the main controls on mineralization?
- Where is the mineralization located within the stratigraphic sequence of the intrusion?
- What are the diagnostic features of PGE mineralization within sections of drill core?

This report presents preliminary results of reconnaissance geological mapping and lithogeochemical sampling conducted in the summer of 2011, together with a review of previous geochemical data compiled by the Manitoba Geological Survey. The aim is to address a fundamental question relating to the economic potential of the Mayville intrusion: Is the intrusion derived from appropriate magma(s) and emplaced in a geological setting favourable for the formation of a base- and precious-metal ore deposit? In order to address this question, it is necessary to investigate the temporal, spatial and petrogenetic relationships among the various intrusive phases within the Mayville intrusion by means of geological mapping,

geochronological determinations and evaluation of the geochemical characteristics.

A petrogenetic model is presented that suggests the Mayville intrusion may have been formed by the injection of multiple batches of magma from a fractionating magma chamber, in which assimilation and fractional crystallization of tholeiitic magma(s) derived from a high degree of partial melting of a depleted mantle source beneath thin (approximately 21 km) lithospheric crust. During emplacement of each batch of magma, assimilation and fractional crystallization may have taken place to some extent. Sulphide saturation, segregation and accumulation may have resulted in PGE-Ni-Cu concentration and mineralization of the mafic–ultramafic rocks, particularly in the basal part of the Mayville intrusion and/or in the contact and transitional zones between different phases in the lower parts of the intrusion. Although differentiation and crustal contamination may result in sulphide saturation in the residual magmas, an external sulphur source would be required to trigger sulphide saturation to produce metal mineralization; the identity of such a source remains, so far, problematic. Redox conditions during the evolution of the magma may have varied from reduced to relatively oxidized conditions, which facilitated crystallization and accumulation of the chromite that is locally concentrated in chromitiferous bands or zones within the intrusion. Based on this model, the most likely settings for PGE-Ni-Cu-(Cr) mineralization in the Mayville intrusion appear to be 1) the basal part of the intrusion; 2) transitional zones between different intrusive phases; 3) at contacts between the different phases; and 4) at the basal contact of the Mayville intrusion, where sulphide minerals may have accumulated if they were not remobilized by later geological events.

Introduction

Nickel–copper–platinum group element–chromium commodities are recovered from a wide range of mineral-deposit types and geological environments associated with igneous rocks of mafic to ultramafic composition, and are therefore primarily of magmatic origin. Mafic–ultramafic igneous bodies are well-recognized in the Bird

¹ Geological Survey of Canada, 490, rue de la Couronne, Québec, Québec G1K 9A9

River greenstone belt (BRGB); intrusions such as the Bird River Sill and the Mayville intrusion contain Ni-Cu sulphide deposits and stratiform chromitite and PGE occurrences (Figure GS-12-1) that have been studied for several decades (Trueman, 1971, 1980; Macek, 1985a, b; Theyer, 1986, 1991, 2003; Ashwal, 1993; Hulbert and Scoates, 2000; Peck et al., 1999, 2000, 2002; Gilbert, 2006, 2007; Gilbert et al., 2008; Good et al., 2009).

Recent exploration programs indicate that a mineralized portion of the Mayville intrusion (i.e., the M2 deposit on the Mayville property) has an NI 43-101 open-pit mineral resource (indicated category) consisting of 9.2 million tonnes averaging 0.61% Cu, 0.23% Ni and 0.43 g/t combined precious metals (Pd+Pt+Au; Mustang Minerals Corp., 2011). More recently, Mustang Minerals also intersected a significant PGE-mineralized zone containing 9.5 g/t Pt+Pd over 9.15 m (diamond-drill hole MAY11-07; Mustang Minerals Corp., 2011), similar to the mineralization style of stratabound PGE-enriched sulphide- and chromite-bearing layers, as described by Hoatson (1998). In addition to the Mayville intrusion, the Bird River Sill (BRS) contains significant Ni-Cu-(PGE) mineralization and hosts two past-producing Ni mines (i.e., Maskwa

West and Dumbarton mines; Trueman and Turnock, 1982). These two mines have recently been re-evaluated and found to still contain 9.6 Mt of ore (probable reserve category) averaging 0.54% Ni, 0.11% Cu, 0.34 g/t Pd and 0.09 g/t Pt (Mustang Minerals Corp., 2011). Furthermore, Scoates et al. (1989) described the PGE-enriched layer within the ultramafic portions of the BRS as traceable for 800 m along the strike of the sill and ranging from tens of centimetres to 3 m in thickness. A number of samples from the PGE-enriched layer in the BRS contain 1.0–2.5 g/t combined Pt+Pd (Cabri and Laflamme, 1988; Scoates et al., 1989).

The BRGB contains other mineral commodities, such as 1) a stratiform chromite deposit in the BRS and significant chromite mineralization in the Mayville intrusion (Trueman and Turnock, 1982; Watson, 1985), 2) potential volcanogenic massive sulphide (VMS)-style Cu-Zn mineralization (C. Galeschuk, pers. comm., 2011), 3) intrusion-related Au mineralization, and 4) a world-class Ta and Cs deposit associated with a granitic pegmatite at the TANCO mine (Černý et al., 1981). It has thus become a key geological belt for mineral exploration. Ultimately, its prime location between two continental cratonic blocks (North Caribou Superterrane and Winnipeg River Subprovince; Figure GS-12-1) will lead to new insights on the overall understanding of the tectonic evolution of this part of the Superior Province in Manitoba. (e.g., Beaumont-Smith et al., 2003; Percival et al., 2006b; Anderson, 2007; Percival, 2007; Corkery et al., 2010), as well as larger scale studies on geodynamic processes involving the assemblage of terranes within the Archean craton (e.g., Hoffman, 1988; Böhm et al., 2000; Burke, 2011).

Following the recent multidisciplinary regional bedrock geological mapping project (2005–2008) within the southern arm of the Neoarchean BRGB (Kremer and Lin, 2006; Gilbert, 2006, 2007; Gilbert et al., 2008; Mealin, 2008; Duguet et al., 2009), the Manitoba Geological Survey (MGS) carried out a reconnaissance geological mapping and lithogeochemical sampling program in the summer of 2011 on the northern arm of the BRGB, which hosts the Mayville mafic–ultramafic intrusion. This paper provides a review and evaluation of existing lithogeochemical data compiled by MGS, to assist with planning a detailed geological mapping project for next field season. The paper also briefly addresses fundamental questions related to the metallogeny of the Mayville intrusion, such as the nature of the magma(s), the rock- and ore-forming processes, the geological and geodynamic environment of the Mayville intrusion and, finally, some economic considerations.

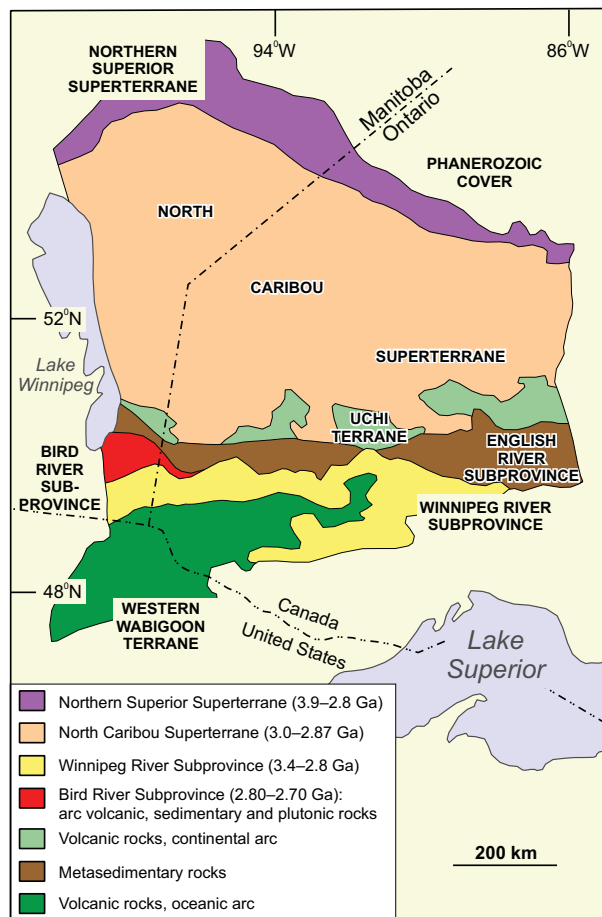


Figure GS-12-1: Simplified geology of the western Superior Province, showing the location of the Neoarchean Bird River greenstone belt (BRGB; after Gilbert, 2007).

Geological setting

The Bird River Sill (BRS) and the Mayville intrusion are layered mafic–ultramafic intrusions that were

emplaced, respectively, in the southern and northern arms of the Neoarchean BRGB, which is situated between the English River and Winnipeg River subprovinces of the Superior Province (Figure GS-12-1; Peck et al., 2002; Gilbert et al., 2008). The BRGB is an exposed part of an approximately 150 km long, east-trending supracrustal belt that extends from Lac du Bonnet in the west to Separation Lake (Ontario) in the east, where it is termed the ‘Separation Lake greenstone belt’ (Percival et al., 2006). Regional aeromagnetic data and Nd-isotope evidence suggest that the BRGB extends westward beneath the Paleozoic sedimentary cover for at least 300 km (Stevenson et al., 2000; Percival et al., 2006a). Investigations of the complex history of deformation, tectonism, metamorphism, magmatism and associated mineralization in the southern part of the BRGB (Percival, 2007; Duguet et al., 2009) have shown it to be in a key position for studies of crustal tectonic processes and the geodynamics of ancient cratons in terms of modern concepts of plate tectonics (e.g., Burke, 2011). These studies have also indicated that the greenstone belt is a prospective area for base metals (Ni, Cu, Cr), precious metals (PGE, Au) and rare metals (Ta, Cs, Li).

Bird River Sill (BRS)

The Bird River Sill (BRS) is a differentiated, layered mafic–ultramafic intrusion, at least 15 km long and 0.8 km thick, that occurs as fault-disrupted subconcordant igneous bodies, trending roughly east and emplaced near or at the contact between the Northern mid-ocean-ridge basalt (MORB)-type formation and the Peterson Creek Formation. The greenstone belt consists mainly of ca. 2.73 Ga arc-type volcanic rocks divided into north and south panels by the relatively younger, turbiditic Booster Lake Formation ($<2712 \pm 17$ Ma; Gilbert, 2006). Mid-ocean-ridge basalt-type volcanic rocks extend along both panels that, although lithologically and geochemically similar, are unlikely to be parts of the same stratigraphic unit; hence, these basaltic formations are termed the ‘Northern MORB-type’ and ‘Southern MORB-type’ formations (Gilbert et al., 2008), respectively.

The Bird River Sill is a layered mafic–ultramafic intrusion that is well-known as the repository of Canada’s most significant chromite resources before the discoveries of the world-class chromite deposits in the McFaulds Lake area of northern Ontario (Metsaranta and Houlé, 2011). It has been studied extensively over the years, a reflection of the overall quality of the exposure and its accessibility, by several workers who established the internal stratigraphy of the sill (Trueman, 1971; Scoates, 1983; Williamson, 1990; Mealin, 2008). The stratigraphy was defined at the Chrome property, which contains the best exposed segment of the Bird River Sill, and is subdivided into three

main magmatic series: ultramafic, transition and mafic. The ultramafic series is composed predominantly of layered dunite, peridotite and chromite; the transition series comprises mainly peridotite with lesser gabbroic rocks; and the mafic series consists predominantly of gabbroic rocks that vary in composition from gabbro and leucogabbro to anorthositic gabbro, with some trondhjemite horizons. The intent here is not to describe in detail the internal stratigraphy, so the reader is referred to previous work, such as Williamson (1990) and Mealin (2008).

Mayville intrusion

The Mayville intrusion is a layered mafic–ultramafic intrusion, at least 10 km long and 1.1 km thick, that occurs as a sill or lopolith trending roughly westwards within the northern arm of the BRGB and is cut by a set of late north-northwest- and northeast-trending faults. The geological context of the northern arm has been described by Macek (1985a, b), but it is not as well constrained as that of the southern arm, which was investigated more recently by the MGS (Gilbert et al., 2008). The Mayville intrusion is emplaced between mafic volcanic rocks similar to the Northern MORB-type formation in the southern arm (Gilbert et al., 2008) to the south, and a composite granitic complex consisting of gneissic rocks and granitoid rocks to the north (Figure GS-12-2; Macek, 1985a, b; Peck et al., 1999; Theyer, 2003; Gilbert, 2006, 2007; Gilbert et al., 2008). The intrusion can generally be divided into two major zones: a lower heterolithic breccia zone and an upper anorthosite to leucogabbro zone. Mafic volcanic xenoliths are not uncommon in the basal part of the lower zone, whereas gneissic and granitoid fragments are evident in the upper part of the upper zone (Peck et al., 1999; Theyer, 2003). Regional metamorphism has affected both the Mayville intrusion and the mafic volcanic hostrocks, which are metamorphosed to greenschist or lower amphibolite facies (Macek, 1985b; Peck et al., 1999, 2002; Theyer, 2003). A broad range of rock types is present in the Mayville intrusion, including anorthosite, leucogabbro, gabbro, melagabbro and pyroxenite;² despite being metamorphosed, these rocks display well-preserved magmatic textures. Massive chromitite layers and/or bands, ranging from a few centimetres to 2 m in width and commonly associated with thinly layered peridotite and/or inclusion-rich peridotite, are present in the lower part of the Mayville intrusion (Hiebert, 2003; Mackie, 2003). Penetrative foliation is locally evident within the intrusion, typically associated with shear zones.

Field observations in 2011 confirmed that the Mayville intrusion can be subdivided into two major zones, a lower heterolithic breccia zone (HBZ) and an upper anorthosite to leucogabbro zone (ALZ), as described previously (Figure GS-12-3; Peck et al., 1999, 2002; Hiebert,

² The prefix ‘meta-’ for these rock types is omitted in this report for simplicity.

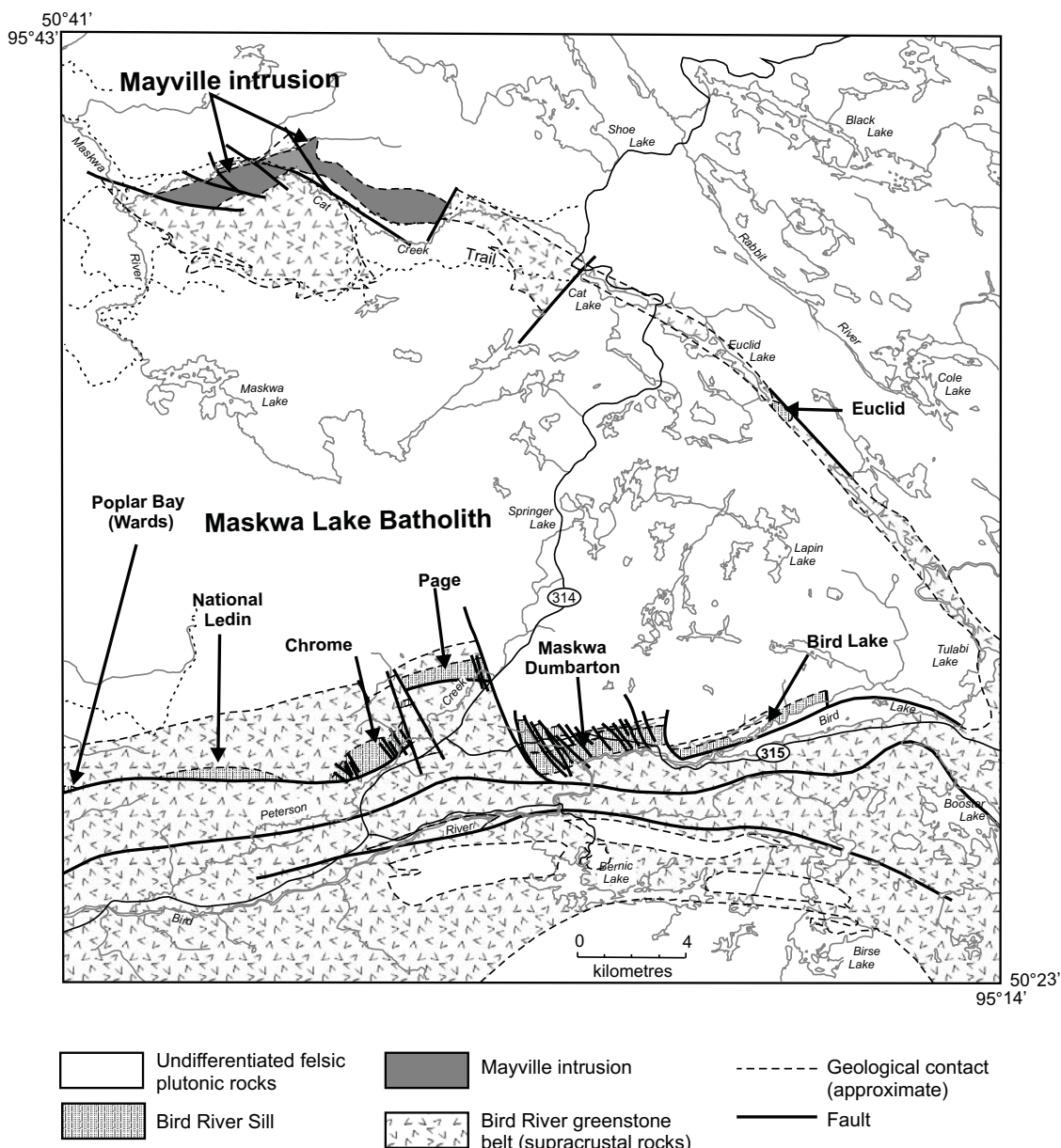


Figure GS-12-2: Simplified geology of the Neoarchean Bird River greenstone belt, showing the location of the Mayville mafic-ultramafic intrusion and the Bird River Sill (after Peck et al., 2002).

2003; Theyer, 2003). The basaltic hostrocks south of the intrusion display sporadic north-facing pillows (Figure GS-12-4a).

Heterolithic breccia zone

The heterolithic breccia zone (HBZ) is composed of diverse rock types, including medium- to coarse-grained and megacrystic, variably textured melagabbro, gabbro and pyroxenite, as well as various associated pegmatitic or megacrystic leucogabbro and anorthosite phases that occur as irregular pods, patches, veins and layers ranging up to 100 m in thickness. Basaltic xenoliths from the country rocks occur in the lower part of the HBZ, and irregular

leucogabbro to anorthosite fragments (Figure GS-12-4b) are locally evident elsewhere in this zone. As an example, the most southerly (inferred basal) HBZ appears to have been emplaced later than the ALZ because the HBZ contains rock fragments, such as leucogabbro and anorthosite, that appear to have been derived from the ALZ. The HBZ is also locally intruded by fine- to medium-grained gabbroic to quartz-bearing gabbroic dikes (Figure GS-12-4f). These dikes contain rare scattered sulphide disseminations. Sulphide minerals (mainly pyrrhotite with minor chalcopyrite±pyrite) occur sporadically in the HBZ as disseminations, net-textured veins and/or locally massive sulphide bands (Figure GS-12-4g, h). Massive chromitite bands and disrupted chromitite-pyroxenite layers

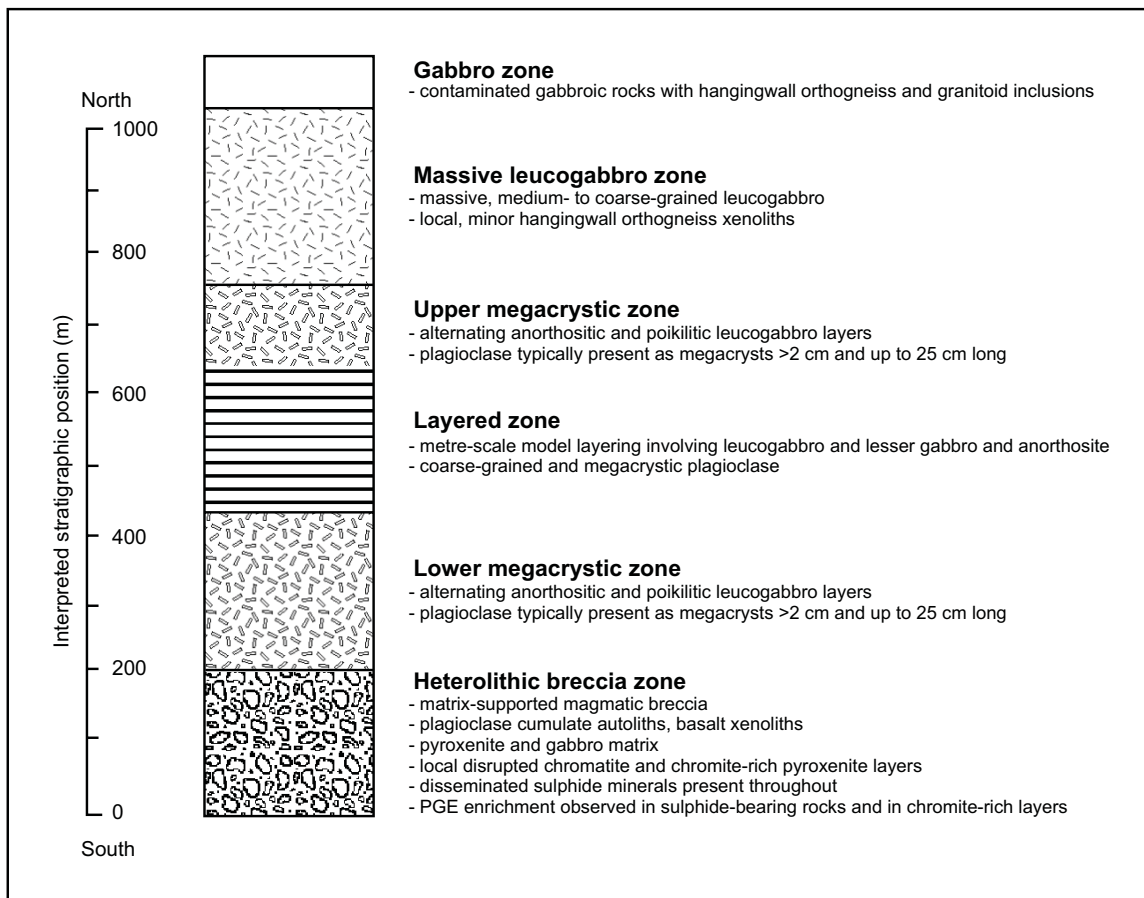


Figure GS-12-3: Schematic stratigraphic section through the Mayville mafic–ultramafic intrusion (after Peck et al., 2002). Note that neither the top and nor the base of the sequence is exposed. Abbreviation: PGE, platinum group element.

are locally present in the middle to upper parts of the HBZ (Peck et al., 2002; Hiebert, 2003).

Anorthosite to leucogabbro zone (ALZ)

According to Peck et al. (1999, 2002), the ALZ can be further subdivided into 1) a lower megacrystic zone, comprising very coarse grained to megacrystic leucogabbro; 2) a layered zone, comprising centimetre- to metre-scale modal and grain-size layering in coarse-grained gabbro, leucogabbro and megacrystic anorthosite (Figure GS-12-4c–e); 3) an upper megacrystic zone, similar to the lower megacrystic zone except for the presence of granitic xenoliths; 4) a massive leucogabbro zone, comprising a lower, coarse-grained poikilitic leucogabbro that is gradational upwards into massive, medium-grained leucogabbro with granitic xenoliths; and 5) a gabbro zone, consisting of medium-grained gabbro with abundant hostrock inclusions of gneiss and granite derived from the roof of the intrusion. The variations in textures and internal layering demonstrate that the Mayville intrusion is a north-facing igneous body with subvertical,

south- to southeast-dipping, overturned primary layering that is subconcordant with surrounding basaltic flows. Stratigraphic details indicate a dynamic intrusive style accompanied by hydrothermal activity, with subsequent major folding that resulted in the present steep to vertical inclination of the mafic–ultramafic sill. Some or all of these processes are likely to have affected and probably remobilized any primary magmatic sulphide mineralization, similar to the mineralization in the BRS that has locally been remobilized during or after emplacement of the intrusion (Murphy and Theyer, 2005; Good et al., 2009).

Geochemical characteristics

A lithogeochemical dataset of 151 whole-rock geochemical analyses from the Mayville intrusion was retrieved from Peck et al. (2000) and reviewed in this study. After removal of numerous samples from the dataset because of their level of alteration,³ the remaining 123 analyses were compiled (Table GS-12-1) to establish the range of geochemical composition of the main rock

³ The data were filtered using a cut-off at 5 wt. % loss-on-ignition (LOI) to remove significantly altered samples (based on the methodology of Rollinson, 1993). In addition, two samples of quartz veins, six samples of sulphur-rich magnetite layers, five samples with SiO₂ greater than 52% and one gabbro sample with SiO₂ lower than 36% were not included in the dataset (Table GS-12-1) used in this study.

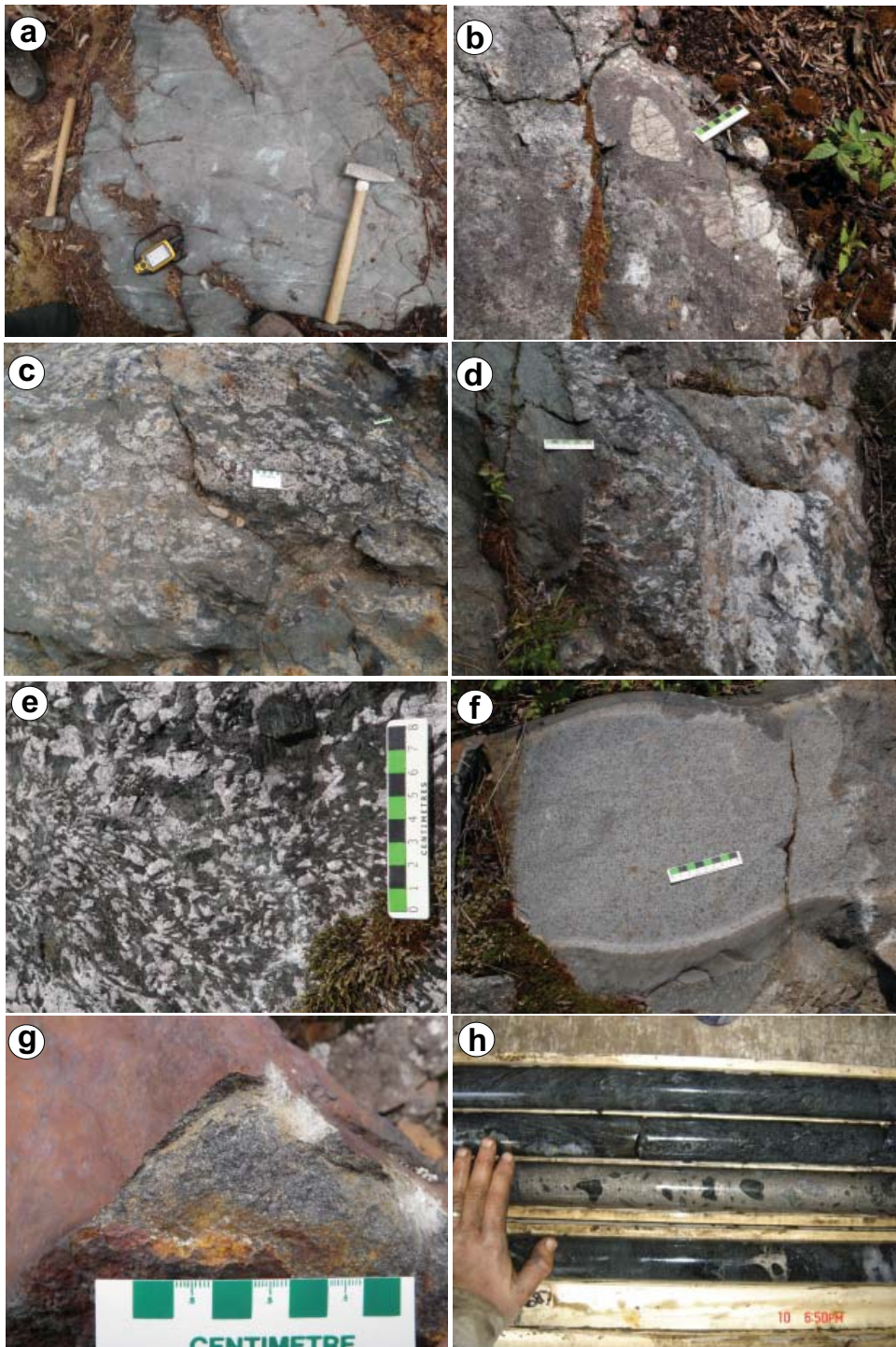


Figure GS-12-4: Field photographs showing lithological features and details of mineralization in the Mayville mafic–ultramafic intrusion and associated country rock: **a)** pillowd basalt of the Northern MORB-type formation, with north-facing pillows discernible in centre and upper left (UTM Zone 15N, 316570E, 5611880N, NAD83); **b)** heterolithic breccia zone containing leucogabbro to anorthosite fragments and disseminated sulphide mineralization (UTM 314064E, 5612456N); **c)** anorthosite to leucogabbro, characterized by subrounded, stretched to irregular aggregates of glomeroporphyritic plagioclase (UTM 315426E, 5612597N); **d)** pyroxenite (left) in sharp contact (fault?) with very coarse grained leucogabbro (right) that is gradational to anorthosite (UTM 314666E, 5612593N); **e)** megacrystic leucogabbro (UTM 315037E, 5612797N); **f)** fine-grained gabbro dike with chilled margin, cutting pyroxenite and gabbro in the heterolithic breccia zone (UTM 314465E, 5612457N); **g)** medium-grained melagabbro with disseminated pyrrhotite and minor chalcopyrite (UTM 316612E, 5611924N); **h)** massive-sulphide layer (pyrrhotite with minor pentlandite and chalcopyrite) in Mustang Minerals Corp. diamond-drill hole May05-04 (drillcore photo courtesy of Mustang Minerals Corp.).

Table GS-12-1: Whole-rock geochemistry for the Mayville mafic–ultramafic intrusion (data from Peck et al., 2000).

Rock type	Anorthosite		Leucogabbro		Gabbro		Melagabbro		Pyroxenite	
	Av.	SD	Av.	SD	Av.	SD	Av.	SD	Av.	SD
n	3		41		65		10		4	
SiO ₂ (wt%) ⁽¹⁾	48.67	0.49	46.13	2.13	47.05	6.20	43.13	3.12	42.59	4.56
TiO ₂	0.24	0.03	0.45	0.22	0.73	0.41	0.33	0.16	0.42	0.24
Al ₂ O ₃	28.70	0.61	23.87	2.33	16.12	4.33	11.20	2.68	9.48	4.75
Fe ₂ O ₃	3.55	0.49	9.18	4.47	13.88	4.25	15.95	2.72	17.14	1.70
MnO	0.05	0.01	0.12	0.03	0.20	0.06	0.22	0.04	0.21	0.07
MgO	2.05	0.65	5.15	2.65	8.93	4.01	21.74	2.46	23.37	2.10
CaO	13.22	0.36	12.75	1.30	11.07	2.39	6.91	1.32	6.35	2.10
Na ₂ O	2.90	0.36	1.98	0.51	1.63	0.65	0.45	0.27	0.43	0.29
K ₂ O	0.57	0.35	0.32	0.21	0.33	0.38	0.08	0.03	0.04	0.01
P ₂ O ₅	0.05	0.01	0.04	0.02	0.06	0.03	0.02	0.00	0.01	0.01
Sum	100		100		100		100		100	
LOI	0.73	0.24	1.23	0.86	1.21	1.11	2.68	1.82	2.21	
S	nd		nd		0.53		0.75	0.34	nd	
Mg# ⁽²⁾	53.4		52.6		56.0		73.0		73.0	
Sc (ppm) ⁽³⁾	8.0	1.0	18.2	6.0	35.1	13.5	18.8	7.5	28.5	14.3
V	143.0	75.4	154.5	91.8	217.3	89.5	251.5	391.7	150.8	32.1
Cr	1845.0	63.6	429.0	1304.9	730.5	1525.2	1344.1	1587.2	365.6	155.0
Co	84.1	49.9	69.1	70.9	99.5	170.2	102.4	40.0	111.7	43.2
Ni	605.5	69.9	921.0	1777.4	1183.8	3423.8	897.8	530.2	685.3	570.5
Cu	242.8	368.4	3243.8	7564.3	2785.8	7309.2	3019.9	4868.5	703.9	862.3
Zn	337.1	389.1	331.0	1206.3	110.5	127.9	183.5	141.3	91.8	59.9
Rb	nd		6.0		3.6	1.2	nd		2.0	
Sr	181.4	149.8	154.3	95.4	101.8	79.2	50.3	63.2	62.2	66.0
Y	6.6	5.4	11.2	6.6	14.7	7.1	8.0	10.3	6.6	2.4
Zr	22.5	13.3	31.0	16.7	40.1	28.7	15.4	4.6	20.3	13.7
Nb	1.3	0.3	2.2	1.6	2.1	1.3	1.1	0.8	0.3	
Ba	55.6	55.9	34.5	28.6	50.4	69.0	9.6	4.4	17.7	6.2
La	1.15	0.39	1.61	0.86	2.78	4.47	1.38	1.98	0.78	0.42
Ce	2.78	1.53	4.08	2.12	6.84	8.79	3.84	6.42	2.06	1.01
Pr	0.43	0.28	0.61	0.32	0.97	1.00	0.62	1.10	0.33	0.14
Nd	2.15	1.48	3.32	1.74	5.02	4.38	3.65	7.06	1.93	0.74
Sm	0.71	0.55	1.09	0.60	1.54	1.01	1.14	2.18	0.61	0.17
Eu	0.48	0.02	0.54	0.18	0.62	0.22	0.34	0.18	0.27	0.12
Gd	0.91	0.77	1.49	0.84	2.03	1.18	1.49	2.83	0.81	0.28
Tb	0.25	0.11	0.30	0.16	0.40	0.19	0.29	0.46	0.16	0.06
Dy	1.66	0.70	1.84	1.11	2.42	1.23	1.43	2.12	0.99	0.47
Ho	0.35	0.14	0.40	0.24	0.54	0.25	0.31	0.40	0.22	0.10
Er	1.06	0.45	1.19	0.75	1.55	0.76	0.79	0.88	0.69	0.29
Tm	0.15	0.07	0.18	0.11	0.24	0.10	0.11	0.10	0.11	0.04
Yb	0.95	0.37	1.12	0.71	1.45	0.69	0.64	0.42	0.72	0.21
Lu	0.14	0.05	0.17	0.11	0.23	0.10	0.09	0.05	0.13	0.01
Hf	0.69	0.21	0.80	0.47	1.09	0.74	0.31	0.08	0.58	0.25
Th	<0.1		0.20	0.11	0.52	1.05	1.07	1.37	0.14	0.10
U	<0.1		0.11		0.28	0.33	0.10		nd	
Se	1.98		4.24	6.66	15.92	26.28	2.52		2.01	
Te	0.67		1.30	1.29	5.54	12.29	1.17		0.86	
Au (ppb)	6.3	0.6	49.7	76.8	66.3	138.6	8.0	10.2	8.3	4.9
Pt	67.3	46.7	62.4	110.0	40.6	39.6	41.3	19.2	37.8	31.1
Pd	164.7	109.5	149.4	168.0	128.7	157.0	68.2	51.9	139.3	124.4

⁽¹⁾ major-element concentrations are in wt. % and are normalized to 100% volatile-free

⁽²⁾ Mg# = molecule MgO / (MgO + FeO'); FeO' = FeO + 0.8998Fe₂O₃

⁽³⁾ trace-element concentrations are in ppm except for Au, which is in ppb

Abbreviations: Av., average; n, number of samples used in averaging; nd = not determined; SD, standard deviation

types of the Mayville intrusion. In addition, new samples were collected in 2011 (analytical results are pending). A petrographic investigation will be carried out on 17 polished thin sections that are currently in preparation.

Major elements

The Mayville intrusion consists of two groups of rocks, based on SiO_2 and MgO contents: mafic and ultramafic (Table GS-12-1; Figure GS-12-5). The mafic group includes anorthosite (average SiO_2 of 48.67%,⁴ MgO 2.05%, Mg# 53.4⁵), leucogabbro (46.13%, 5.15%, 52.6) and gabbro (47.05%, 8.93%, 56.0), whereas the ultramafic group contains melagabbro (43.13%, 21.74%, 73.0) and pyroxenite⁶ (42.59%, 23.37%, 73.0).

Based on the dataset, the Mayville intrusion is geochemically a composite and relatively evolved mafic-ultramafic intrusion, comparable to Archean megacrystic anorthosite suites (Ashwal, 1993).

The chemical data from most samples ($n = 123$) used in this study display a tholeiitic trend in the alkalis-iron-magnesium (AFM) diagram (Figure GS-12-6), characterized by conspicuous FeO^T enrichment.⁷ This requires relatively reduced redox conditions to retain ferrous iron in the magma, which is favourable for sulphide formation if it is saturated in the magma. However, the anorthosite and a few leucogabbro samples fall into the

calcalkaline field. This can be explained by early crystallization of calcic-plagioclase crystals that would float to concentrate and form one or more anorthosite layers at the top of a magma chamber, or could be attributed to assimilation and crustal contamination. The effect of crustal contamination on the chemistry of the Mayville intrusion is consistent with the discrimination results from plotting the parameters s versus t (plot not shown). The parameter s , termed the ‘Rittmann serial index’, is defined as $(\text{Na}_2\text{O} + \text{K}_2\text{O})^2/(\text{SiO}_2 - 43)$; t , referred as the Gottini index, is defined as $(\text{Al}_2\text{O}_3 - \text{Na}_2\text{O})/\text{TiO}_2$ (Yang et al., 2008).

The chemical relationships between various rock types in the Mayville intrusion are well displayed in the Al_2O_3 versus $\text{Mg}^{\#}$ diagram (Figure GS-12-7), in which a trend of assimilation and fractional crystallization (AFC) is clearly defined. The $\text{Mg}^{\#}$ tends to decrease with progressive fractionation, concurrent with increasing Al_2O_3 . The broad scatter of data for gabbro and leucogabbro is interpreted as evidence for crustal contamination of the magmatic source. The absence of compositions analogous to residual mantle peridotite in this diagram is noteworthy and rules out the possibility that the Mayville intrusion is a part of ophiolite suite. In addition, probable cumulate rocks, such as pyroxenite and melagabbro, may be present, representing basal parts of the intrusion that were disrupted and entrained by a late pulse of magma.

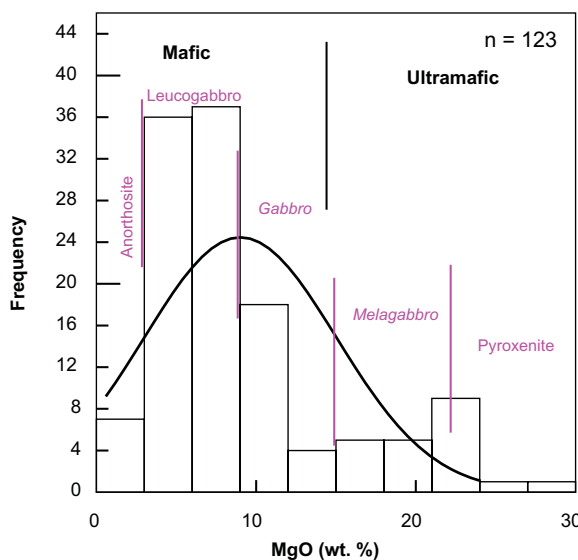


Figure GS-12-5: Histogram of MgO contents (wt. %) for the Mayville intrusion, showing a relatively evolved mafic-ultramafic intrusion.

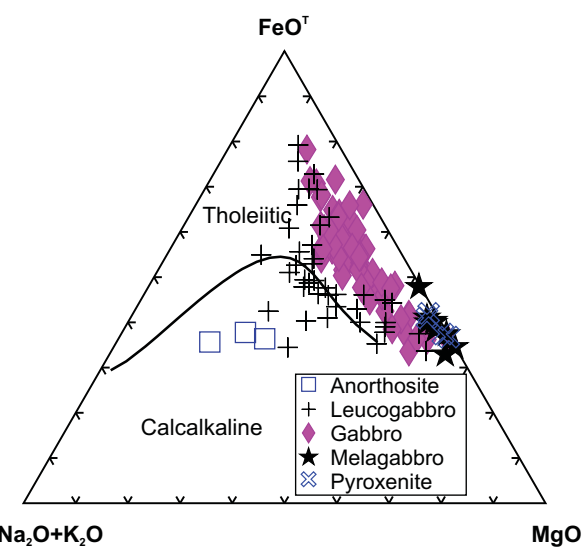


Figure GS-12-6: AFM diagram for the Mayville intrusion, showing the division of tholeiitic and calcalkaline magmas (after Irvine and Baragar, 1971). Abbreviations: A, $\text{Na}_2\text{O} + \text{K}_2\text{O}$; FeO^T , total Fe as FeO ; M, MgO . All values in wt. %.

⁴ Analytical data are quoted as wt. %; the sequence of values in the data string shown for anorthosite applies to subsequent rock types.

⁵ Mg# = molecule $\text{MgO} / (\text{MgO} + \text{FeO}^T)$; $\text{FeO}^T = \text{FeO} + 0.8998 \text{ Fe}_2\text{O}_3$.

⁶ The terminology used for rock types in Peck et al. (2000) is retained in this report, but the terms of the IUGS Subcommission on the Systematics of Igneous Rocks are recommended (Le Maitre et al., 2002).

⁷ $\text{FeO}^T = \text{FeO} + 0.8998 \text{ Fe}_2\text{O}_3$

Trace elements

Mafic and ultramafic rocks in the Mayville intrusion are characterized by low Zr/TiO_2 and Nb/Y ratios (Table GS-12-1), typical for the subalkaline series (Figure GS-12-8) and consistent with a magmatic-arc setting (Syme, 1998). Low ratios of Nb/Y , Zr/TiO_2 and $Zr/P_{2}O_5$ suggest the Mayville intrusion has a tholeiitic rather than calcalkaline petrogenetic affinity. These three ratios involving high-field-strength elements (HFSE) correlate positively with one another and, although the data points are fairly scattered, indicate that magmatic evolution was associated with a defined AFC trend, as described above (Figure GS-12-7). Only a few gabbroic samples plot outside the basalt field in Figure GS-12-8, probably due to the effect of crustal contamination on their composition. Because the HFSE are stable and would not readily be remobilized by late metamorphism and alteration, the classification of the Mayville intrusion rocks described here is considered reliable, and also consistent with the patterns in the AFM diagram (Figure GS-12-6).

It has long been recognized that the chemical compositions of a volcanic rock can be altered by hydrothermal processes, chemical weathering and/or metamorphism (e.g., Rollinson, 1993; Syme, 1998). In order to address

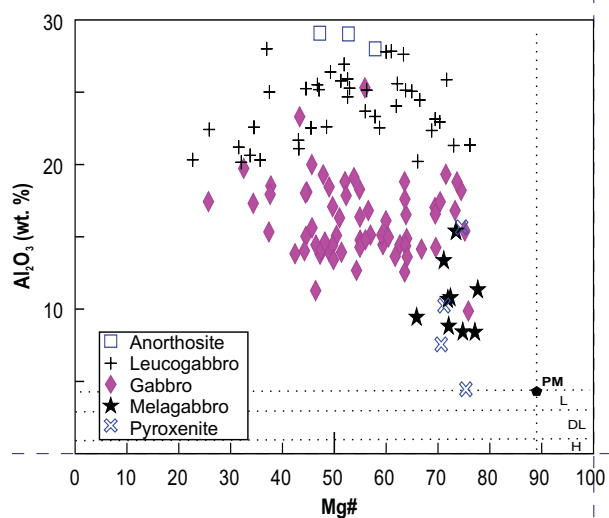


Figure GS-12-7: Plot of $Mg\#$ vs. Al_2O_3 for mafic–ultramafic rocks in the Mayville intrusion. The boundaries of residual mantle peridotite, taken from Peltonen et al. (1998), are based on Al_2O_3 contents: harzburgite (H) < 1%; 1% < depleted lherzolite (DL) < 3%; and 3% < lherzolite (L) < 4.45%. The $Mg\#$ of the residual mantle rocks should be higher than that of primitive mantle (89.3). The Al_2O_3 contents of cumulate ultramafic rocks should be higher than the primitive mantle (4.45%), but with lower $Mg\#$ (<89.3). It should be noted that PM position is approximate, and can vary as a result of alteration. Note that serpentinization of peridotite can result in uptake of up to 15% water; at that level, the Al_2O_3 boundaries for the mantle residues (H , DL , L) would be lowered to 0.8, 2.5 and 3.8%, respectively. Abbreviations: $Mg\#$ = molecule $MgO / (MgO + FeO^T)$; $FeO^T = FeO + 0.8998 Fe_2O_3$; PM, primitive mantle (McDonough and Sun, 1995).

this problem, Hattie et al. (2007) proposed a new Th versus Co discrimination diagram (Figure GS-12-9). Most of the samples from the Mayville intrusion plot in the island-arc tholeiite (IAT) field in this diagram, and are basaltic in composition. In summary, the parental magma(s) of the Mayville intrusion was/were subalkaline and tholeiitic, and may have been contaminated by crustal material during emplacement into a magmatic-arc environment, consistent with the interpretation based on the AFM and Zr/TiO_2 versus Nb/Y discrimination diagrams (Irvine and Baragar, 1971; Pearce, 1996; Syme, 1998).

Chondrite-normalized, rare earth element (REE) patterns of the major rock types in the Mayville intrusion (Table GS-12-1) are similar to one another; they display flat to slightly positive slopes with moderate to pronounced Eu positive anomalies (Figure GS-12-10a), except for melagabbro, which exhibits a small negative Eu anomaly. These profiles are parallel or subparallel, except for the melagabbro plot, which intersects the others in some places. The $(La/Yb)_N$ ratios of Mayville rocks are 0.77 (pyroxenite), 0.87 (anorthosite), 1.03 (leucogabbro), 1.37 (gabbro) and 1.56 (melagabbro). These REE characteristics collectively suggest that the Mayville intrusion may have been characterized by multiple batches of magma derived from a common magma chamber where fractional crystallization took place, probably involving all constituent minerals except for plagioclase as fractionating phases. Melagabbro, characterized by a moderate negative Eu anomaly (Figure GS-12-10a), may be an

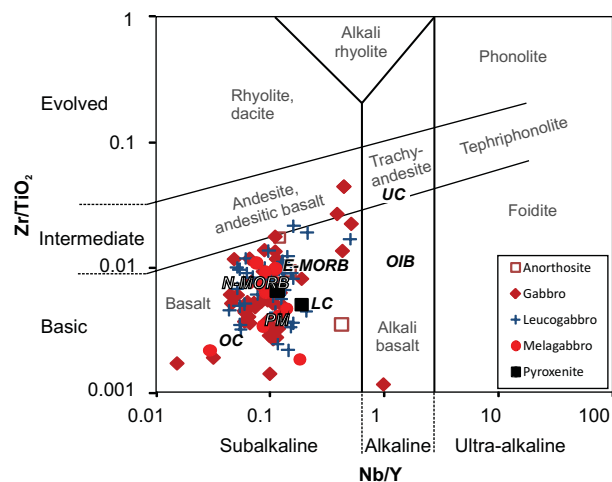


Figure GS-12-8: Plot of Zr/TiO_2 vs. Nb/Y (Pearce, 1996) for the Mayville intrusion, widely used as an immobile element equivalent to the TAS (total alkalis vs. silica) diagram (Rollinson, 1993). The TiO_2 values are quoted in ppm when calculating Zr/TiO_2 ratios. Rock type abbreviations (Sun and McDonough, 1989): PM, primitive mantle; N-MORB, normal mid-ocean-ridge basalt; E-MORB, enriched mid-ocean-ridge basalt; OIB, oceanic-island basalt. Crust abbreviations (Taylor and McLennan, 1985): UC, upper continental crust; LC, lower continental crust; OC, oceanic crust.

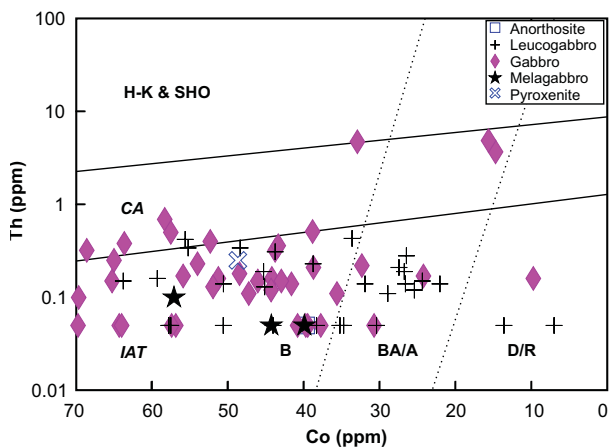


Figure GS-12-9: Plot of Th vs. Co for the Mayville intrusion. The field boundaries are after Hattie et al. (2007). Rock series abbreviations: H-K & SHO, high-K calcalkaline and shoshonite; CA, calcalkaline; IAT, island-arc tholeiite. Rock type abbreviations: B, basalt; BA, basaltic andesite; A, andesite; D, dacite; R, rhyolite.

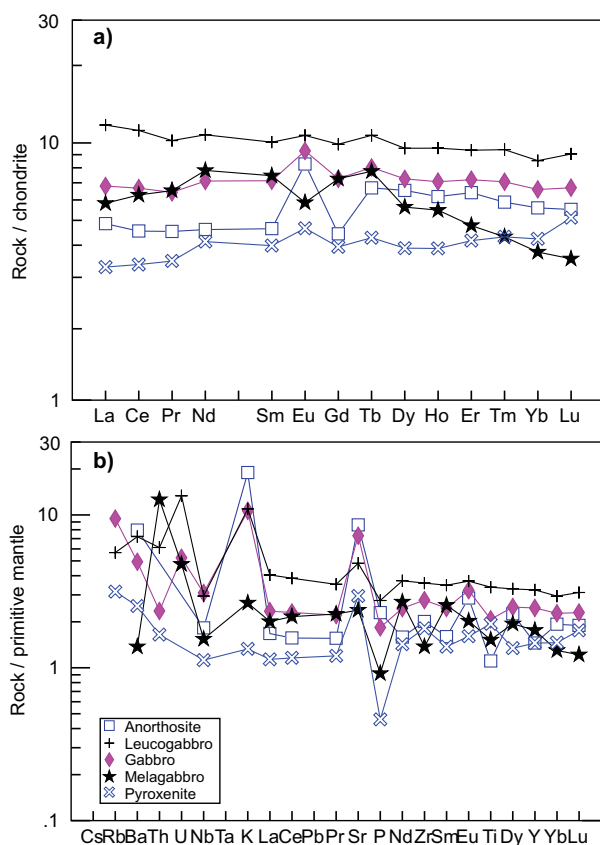


Figure GS-12-10: Chondrite-normalized REE diagram (a) and primitive-mantle-normalized extended element diagram (b) for the various rock types (Table GS-12-1) in the Mayville intrusion. Normalizing values from Sun and McDonough (1989).

exception in this model because it appears to represent a residual phase following fractionation of plagioclase. This is interpreted to indicate that the magma(s) was/were probably derived from a relatively shallow depleted mantle that underwent a high degree of partial melting. Plagioclase may have been absent in the fractionating phases that led to anorthosite, leucogabbro, gabbro and pyroxenite in the Mayville intrusion, but it is present as a constituent mineral in these rocks.

The primitive-mantle-normalized, extended element diagram (Figure GS-12-10b) shows enrichment in Th (and other large-ion lithophile elements [LILE], such as K, Rb, Cs, and Sr), with moderate to pronounced negative Nb, P and Ti anomalies. These profiles are consistent with mafic-ultramafic rocks derived from a magmatic-arc system, where arc-related magmas are generated by decompression melting in the mantle wedge augmented by fluid and/or magma additions from the subducting lithospheric slab (Pearce and Peate, 1995; Tatsumi and Eggins, 1995; Mantle and Collins, 2008). The slab contributed LILE, such as K, Rb, Ba and Sr (as well as Pb), whereas the mantle wedge contributed HFSE, such as Zr, Hf, Ti and Y, as well as heavy REE, to the arc magmas. A slightly positive Ti anomaly in pyroxenite (Figure GS-12-10b) may be due to the accumulation of Ti-Fe oxide minerals, such as ilmenite and/or rutile (Hiebert, 2003).

Discussion

Age constraints

Although the absolute age of the Mayville intrusion is not yet known, field relations indicate that it is younger than contiguous basaltic rocks to the south, which are inferred to be part of the Northern MORB-type formation; this formation predates the 2744.7 ± 5.2 Ma age of the BRS, established in the southern arm of the belt (Wang, 1993). An upper age limit for the Mayville intrusion is provided by the 2832 Ma age (Gilbert et al., 2008) of a granodiorite phase in the Maskwa Lake Batholith (Figure GS-12-2), which appears to predate the MORB-type volcanism. The diverse rocks within the chaotic HBZ of the Mayville intrusion locally contain basaltic fragments and/or xenoliths akin to the Northern MORB-type formation, and fragments of leucogabbro and anorthosite from the overlying ALZ, which contains xenoliths of granitoid rocks and related gneiss. The HBZ is locally cut by late quartz-bearing gabbroic dikes.

Tectonic setting

Although the tectonic settings of polydeformed and metamorphosed Archean greenstone belts are difficult to establish unambiguously, some insights can be deduced from tectonic-discrimination diagrams. However, these diagrams should be treated with caution because they do

not provide unequivocal confirmation of a former tectonic environment but, at best, suggest an affiliation (Rollinson, 1993). Based on such diagrams, the magma source for the Mayville intrusion is subalkaline and exhibits a tholeiitic affinity, typical of a magmatic-arc or island-arc setting (Figure GS-12-9). On the TiO_2/MnO versus Mg# plot (Figure GS-12-11a), most Mayville intrusion rocks plot exclusively in the volcanic-arc field. In the Zr/Y versus Zr discrimination diagram (Figure GS-12-11b) of Pearce (1983), however, these samples plot in both the oceanic- and continental-arc fields, consistent with a transition from oceanic-arc to continental-arc environment, as suggested by Gilbert (2007) and Gilbert et al. (2008). Distinctive differences in the geochemical affinity and diagnostic-element ratios exist between volcanic rocks in the BRGB north and south panels, respectively. Discriminant plots, such as Th/Ta versus Yb (Gorton and Schandl, 2000), Zr versus TiO_2 (Syme, 1998) and Th/Nb versus Y (Syme et al., 1999), indicate that the north panel rocks may represent a convergent, subduction-type setting, whereas the south panel rocks are consistent with a transition from a convergent to an extensional setting and can therefore reflect an incipient arc-rifting environment.

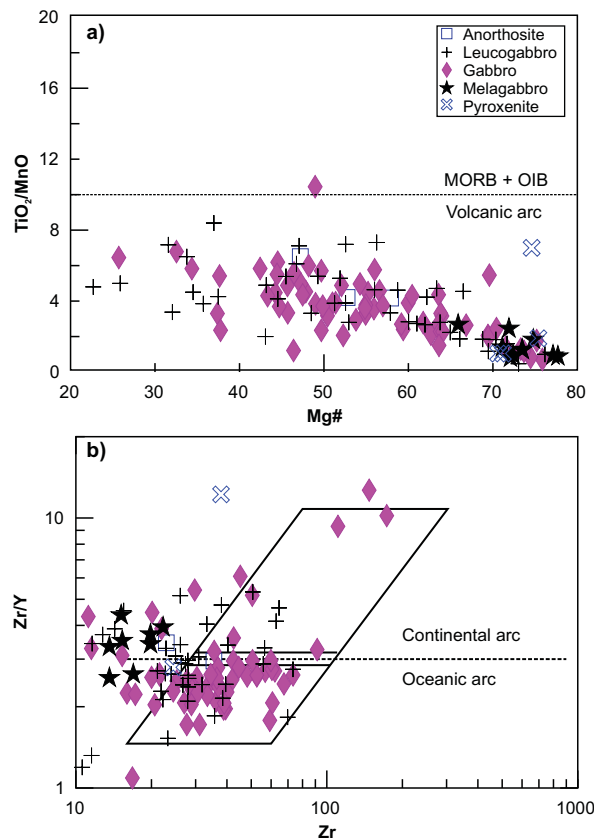


Figure GS-12-11: Plots for the Mayville intrusion of **a)** TiO_2/MnO ratio vs. Mg# (approximate line separating volcanic-arc from MORB and OIB fields from Mullen, 1983), and **b)** Zr/Y vs. Zr diagram (division between continental arc and oceanic arc from Pearce, 1983). Abbreviations: Mg# = $\text{MgO} / (\text{MgO} + \text{FeO}')$; MORB, mid-ocean-ridge basalt; OIB, oceanic-island basalt.

Additional evidence for the interpretation of tectonic setting consists of crustal-thickness estimation based on an empirical relationship between Moho depth (i.e., crustal thickness) and the maximum Ce/Y ratio of subalkaline basalt suites derived from volcanic-arc settings in modern environments, where seismically defined Moho depth measurements are available (Mantle and Collins, 2008). The relationship of Moho depth as an exponential function of the maximum Ce/Y ratios with a correlation coefficient (R^2) of 0.90 is reorganized and expressed using natural logarithm treatment as

$$D (\pm 3 \text{ km}) = 18.1 \times \ln(\text{Ce/Y})_{\max} + 21.6, \quad (1)$$

where D denotes Moho depth in kilometres; $(\text{Ce/Y})_{\max}$ is the maximum value of a subalkaline basalt suite from a volcanic-arc setting, with 44–53% SiO_2 , $\text{MgO} > 4\%$, and $\text{LOI} < 4\%$. Mantle and Collins (2008) indicated that the accuracy of the resulting thickness estimates is ± 3 km for crustal thicknesses of 10–50 km.

This correlation is consistent with the findings of Plank and Langmuir (1988) that crustal thickness is reflected by the major-element composition of arc basalt. This relationship was applied to New Zealand, part of the eastern Gondwana margin through much of the Phanerozoic, and showed that higher Ce/Y ratios in arc basalt correspond to two periods of crustal thickening associated with the Gondwanide orogeny (Mantle and Collins, 2008). Conversely, low Ce/Y ratios in basalt correlate with periods of extension that led to crustal thinning in eastern Gondwana (Mantle and Collins, 2008). Interpretation of the Ce/Y ratio was also successfully used to estimate crustal thickness of the Blue Mountain province in northeastern Oregon, the results suggesting that the Dixie Butt arc (ca. 162 Ma) rests on thin juvenile crust approximately 23 km thick (Schwartz et al., 2011).

The maximum Ce/Y ratio in subalkaline basalt of the Northern MORB-type formation (footwall of the Mayville intrusion) is 0.98 (Gilbert, unpub. data, 2011), corresponding to a Moho depth of 21.3 km according to the model of Mantle and Collins (2008). This is consistent with a thinner crust (relative to that beneath the volcanic front of the BRGB arc), possibly related to an extensional setting such as incipient arc rifting in a back-arc environment, as pointed out by Gilbert (2007) and Gilbert et al. (2008). Despite the fact that Ni-Cu-(PGE) mineralization occurs in a wide range of tectonic settings (e.g., divergent, convergent, meteorite impact), most economic deposits occur in rift-related settings (i.e., extension) where a crustal thinning occurred. This situation is inferred for the BRGB from the geochemical signatures of both the intrusion and its country rocks, and also by the crustal-thickness calculation based on the model of Mantle and Collins (2008). As proposed by Gilbert et al. (2008), the Mayville intrusion may be an expression of a magmatic-arc system represented by the BRGB that could have evolved from an oceanic-arc to a continental-arc setting

during convergence between the North Caribou Superterane to the north and the Winnipeg River Subprovince to the south, ca. 2.75–2.70 Ma (Figure GS-12-1).

Large igneous provinces are characterized by bimodal magmatism associated with continental rifting caused by mantle plumes, and may have hosted large- to giant-size magmatic Ni-Cu-PGE ore deposits (e.g., Noril'sk, Jinchuan, Bushveld; Zhang et al., 2008). Volcanic and intrusive packages are present in magmatic-arc systems throughout the geological record, and may have hosted small- to mid-sized magmatic Ni-Cu-PGE deposits (e.g., Tati and Selebi-Phikwe belts, eastern Botswana; Maier et al., 2008).

Petrogenetic model

Geochemical signatures of the Mayville intrusion, coupled with field relationships such as the chaotic nature of the heterolithic breccia zone and the presence of fragments of leucogabbro and anorthosite from the overlying ALZ, which contains xenoliths of granitoid rocks and related gneiss, suggest that the Mayville intrusion may have been formed by multiple injections of tholeiitic magma that underwent fractional crystallization and some assimilation of the country rocks. A similar scenario was proposed by Mackie (2003). The magma generated beneath a relatively thin (<25 km) lithosphere may have begun to crystallize calcic plagioclase, which then rose and segregated to form one or more anorthositic layers. These layers may subsequently have been broken up due to gravity instabilities or tectonic setting and, in part, became entrained within batches of late, turbulent magma at or close to the top of the magma chamber.

Fractional crystallization and assimilation of the country rocks concurrent with magmatic emplacement would be an important requirement for segregating magmatic Ni-Cu-PGE sulphide mineralization (Lightfoot and Naldrett, 1999; Lesher et al., 2001; Peck et al., 2001). Plots of the Mayville intrusion rocks on the Ni versus Cu/Zr diagram (Figure GS-12-12a) display a trend consistent with sulphide segregation and fractional crystallization, suggesting that the intrusion was saturated with sulphide minerals. This hypothesis is supported by the presence of sulphide minerals as inclusions in early products of fractionation, such as pyroxene (amphibole) and chromite (Hiebert, 2003). Saturation, segregation and accumulation of sulphide minerals may have resulted in PGE-Ni-Cu concentration and mineralization, particularly in the basal part of the intrusion, and in the contact and transitional zones between different phases in the lower portions of the intrusion. Although differentiation and crustal contamination may result in sulphide saturation in the residual magmas, an external source of sulphur appears necessary to trigger sulphide saturation and segregate significant amounts of sulphide mineralization. Although early sulphide saturation in magmas is evident (Hiebert,

2003), an external source for sulphur has not yet been identified.

Economic considerations

The Mayville intrusion hosts a significant amount of Ni-Cu-PGE and PGE-Ni-Cu-(Cr) mineralization that occurs, respectively, as contact-style and as reef-style stratiform magmatic mineralization. Preliminary investigations involving core logging and analytical data show that sulphide-rich mineralization is typically located near the base of the heterolithic breccia zone (HBZ) and basal contact of the intrusion, whereas disseminated sulphide minerals are widespread throughout the HBZ, and transition zones between major rock units may carry significant amounts of PGE.

It is important to discern the relationship between PGE mineralization and fractionation of the host magma in the Mayville intrusion (Figure GS-12-12b), as well as to assess the role of Ni depletion, which has been reported as an effective exploration tool by Lightfoot et al. (1997), Lightfoot and Naldrett (1999) and Lesher et al. (2001). However, the lack of data on the original thickness of the intrusion and the lack of systematic geochemical sampling across the entire intrusion make this impossible.

Investigation of the magmatic architecture of the Mayville intrusion via the physical properties of the intrusive

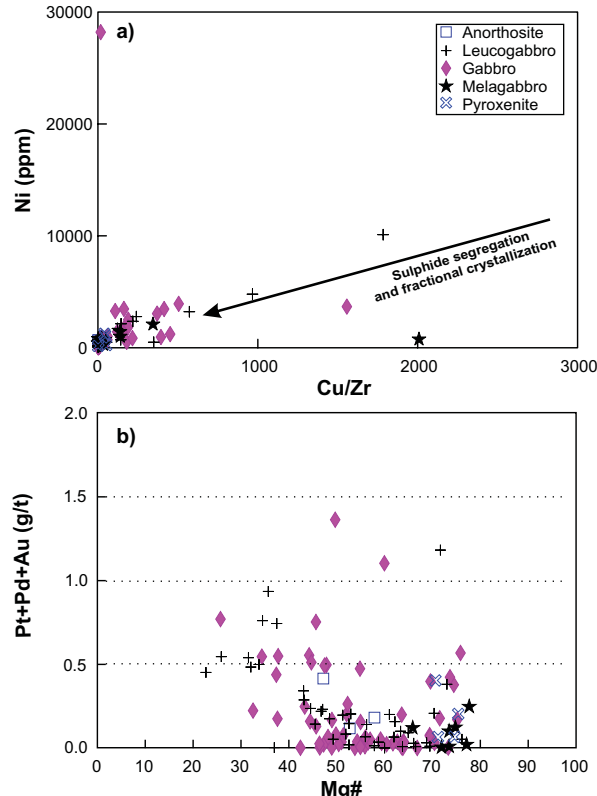


Figure GS-12-12: Plots of Ni (ppm) vs. Cu/Zr (**a**) and noble metals (Pt+Pd+Au in g/t) vs. Mg# (**b**) for the Mayville intrusion.

magma and the surrounding rocks, together with structural and geophysical analysis, may assist in interpreting the mechanism of emplacement (Houlé et al., 2008), as well as identifying the potential location of a feeder and/or magma conduit.

In addition to the Ni-Cu-PGE sulphide mineralization, the Mayville intrusion may host significant chromite mineralization, as suggested by the presence of massive chromitite bands and disrupted chromitite-pyroxenite layers within the HBZ.

Conclusions and future work

In summary, the Mayville intrusion is one of the major layered mafic-ultramafic intrusions in the BRGB. The dominant mafic part is subdivided into two zones: the heterolithic breccia zone and the anorthosite-leucogabbro zone. Based on preliminary analytical results, it is interpreted as an evolved mafic intrusion of tholeiitic affinity that exhibits some contamination signatures. Preliminary assessment of its geochemical characteristics using tectonic discrimination diagrams suggests a magmatic-arc system as the tectonic setting of the intrusion, consistent with that proposed by Gilbert et al. (2008) for the BRGB. The Mayville intrusion hosts one Ni-Cu-(PGE) deposit within the heterolithic breccia zone (M2 deposit) and significant PGE and chromite mineralization.

Detailed geological mapping, together with geochemical and geochronological investigations in the course of this project, are expected to yield new insights into the intrusion's metallogeny, and the potential for base- and precious-metal mineralization associated with mafic-ultramafic intrusions in the BRGB in general and the Mayville intrusion in particular. The study will also address the relationship between Cr and Ni-Cu-PGE sulphide mineralization in these intrusions, as well as the potential to host Fe-Ti-V oxide mineralization. Finally, the study is expected to improve our overall understanding of the geological and tectonic evolution of the BRGB within the Superior Province.

Acknowledgments

The authors thank Mustang Minerals Corp. for providing access to their property and drillcore, in particular C. Galeschuk, A. Dietz and R. Shegelski for their generous assistance in the field and constructive discussion. We thank G. Keller for technical support, L. Chackowsky for providing GIS data, M. Pace for assembling the digital database for a hand-held data acquisition system, B. Lentton and M. McFarlane for digitizing the map data and drafting figures, E. Hunter for locating some key references, and G. Benger and R. Uhruh for handling the samples and preparing polished thin sections. N. Brandson and E. Anderson are thanked for assembling field equipment and providing expediting services.

References

- Anderson, S.D. 2007: Stratigraphic and structural setting of gold mineralization in the Lily Lake area, Rice Lake greenstone belt, Manitoba (NTS 52L11, 14); *in Report of Activities 2007*, Manitoba Science, Technology, Energy and Mines, Manitoba Geological Survey, p. 114–128.
- Ashwal, L.D. 1993: Anorthosites; Springer-Verlag, Berlin, Germany, 422 p.
- Beaumont-Smith, C.J., Anderson, S.D., Bailes, A.H. and Corkery, M.T. 2003: Preliminary results and economic significance of geological mapping and structural analysis at Sharpe Lake, northern Superior Province, Manitoba (parts of NTS 53K5 and 6); *in Report of Activities 2003*, Manitoba Industry, Economic Development and Mines, Manitoba Geological Survey, p. 140–158.
- Böhm, C.O., Heaman, L.M., Creaser, R.A. and Corkery, M.T. 2000: Discovery of pre-3.5 Ga exotic crust at the north-western Superior Province margin, Manitoba; *Geology*, v. 28, p. 75–78.
- Burke, K. 2011: Plate tectonics, the Wilson cycle, and mantle plumes: geodynamics from the top; *Annual Reviews of Earth and Planetary Sciences*, v. 39, p. 1–29.
- Cabri, L.J. and Laflamme, J.H.G. 1988: Mineralogical study of the platinum-group element distribution and associated minerals from three stratigraphic layers, Bird River Sill, Manitoba; CANMET Report 88-1E, 59 p.
- Černý, P., Trueman, D.L., Ziehlke, D.V., Goad, B.E. and Paul, B.J. 1981: The Cat Lake–Winnipeg River and the Wekusko Lake pegmatite fields, Manitoba; Manitoba Energy and Mines, Mineral Resources Division, Economic Geology Report ER80-1, 216 p.
- Corkery, M.T., Murphy, L.A. and Zwanzig, H.V. 2010: Re-evaluation of the geology of the Berens River Domain, east-central Manitoba (parts of NTS 52L, M, 53D, E, 62P, 63A, H); *in Report of Activities 2010*, Manitoba Innovation, Energy and Mines, Manitoba Geological Survey, p. 135–145.
- Duguet, M., Lin, S., Davis, D.W., Corkery, M.T. and McDonald, J. 2009: Long-lived transpression in the Archean Bird River greenstone belt, western Superior Province, south-eastern Manitoba; *Precambrian Research*, v. 174, no. 3–4, p. 381–407.
- Gilbert, H.P. 2006: Geological investigations in the Bird River area, southeastern Manitoba (parts of NTS 52L5N and 6); *in Report of Activities 2006*, Manitoba Science, Technology, Energy and Mines, Manitoba Geological Survey, p. 184–205.
- Gilbert, H.P. 2007: Stratigraphic investigations in the Bird River greenstone belt, Manitoba (part of NTS 52L5, 6); *in Report of Activities 2007*, Manitoba Science, Technology, Energy and Mines, Manitoba Geological Survey, p. 129–143.
- Gilbert, H.P., Davis, D.W., Duguet, M., Kremer, P., Mealin, C.A. and MacDonald, J. 2008: Geology of the Bird River Belt, southeastern Manitoba (parts of NTS 52L5, 6); Manitoba Science, Technology, Energy and Mines, Manitoba Geological Survey, Geoscientific Map MAP2008-1, scale 1:20 000.

- Good, D., Mealin, C. and Walford, P. 2009: Geology of the Ore Fault Ni-Cu deposit, Bird River Sill complex, Manitoba; *Exploration and Mining Geology*, v. 18, p. 41–57.
- Gorton, M.P. and Schandl, E.S. 2000: From continents to island arcs: a geochemical index of tectonic setting for arc-related and within-plate felsic to intermediate volcanic rocks; *Canadian Mineralogist*, v. 38, p. 1065–1073.
- Hattie, A.R., Kerr, A.C., Pearce, J.A. and Mitchell, S.F. 2007: Classification of altered volcanic island arc rocks using immobile trace elements: development of the Th-Co discrimination diagram; *Journal of Petrology*, v. 48, p. 2341–2357.
- Hiebert, R. 2003: Composition and genesis of chromite in the Mayville intrusion: southeastern Manitoba; B.Sc. thesis, University of Manitoba, Winnipeg, Manitoba, 96 p.
- Hoatson, D.H. 1998: Platinum-group element mineralisation in Australian Precambrian layered mafic-ultramafic intrusions; *AGSO Journal of Australian Geology & Geophysics*, v. 17, p. 139–151.
- Hoffman, P.H. 1988: United plates of America, the birth of a craton: Early Proterozoic assembly and growth of Laurentia; *Annual Reviews of Earth and Planetary Sciences*, v. 16, p. 543–603.
- Houlé, M.G., Gibson, H.L., Lesher, C.M., Davis, P.C., Cas, R.A.F., Beresford, S.W. and Arndt, N.T. 2008: Komatiitic sills and multigenerational peperite at Dundonald Beach, Abitibi greenstone belt, Ontario: volcanic architecture and nickel sulfide distribution; *Economic Geology*, v. 103, p. 1269–1284.
- Hulbert, L. and Scoates, J. 2000: Digital map and database of magmatic Ni-Cu±PGE occurrences and mafic-ultramafic bodies in Manitoba; Manitoba Industry, Trade and Mines, Manitoba Geological Survey, Economic Geology Report ER2000-1, CD-ROM.
- Irvine, T.N. and Baragar, W.R.A. 1971: A guide to the chemical classification of the common volcanic rocks; *Canadian Journal of Earth Sciences*, v. 8, p. 523–548.
- Kremer, P.D. and Lin, S. 2006: Structural geology of the Bernic Lake area, Bird River greenstone belt, southeastern Manitoba (NTS 52L6): implications for rare element pegmatite emplacement; *in Report of Activities 2006*, Manitoba Science, Technology, Energy and Mines, Manitoba Geological Survey, p. 206–213.
- Le Maitre, R.W., Streckeisen, A., Zanettin, B., Le Bas, M.J., Bonin, B., Bateman, P., Bellieni, G., Dudek, A., Efremova, S.A., Keller, J., La myre, J., Sabine, P.A., Schmid, R., Sorensen, H. and Woolley, A.R. 2002: Igneous rocks: a classification glossary of terms; Cambridge University Press, Cambridge, 236 p.
- Lesher, C.M., Burnham, O.M., Keays, R.R., Barnes S.J. and Hulbert, L. 2001: Trace-element geochemistry and ore-associated komatiites; *Canadian Mineralogist*, v. 39, p. 673–696.
- Lightfoot, P.C. and Naldrett, A.J. 1999: Geological and geochemical relationships in the Voisey's Bay intrusion, Nain Plutonic Suite, Labrador, Canada; *in Dynamic Processes in Magmatic Ore Deposits and their Application to Mineral Exploration*, R.R. Keays, C.M. Lesher, P.C. Lightfoot and C.E.G. Farrow (ed.), Geological Association of Canada, Short Course Notes 13, p. 1–30.
- Lightfoot, P.C., Hawesworth, C.J., Olshefsky, K., Green, T., Doherty, W. and Keays, R.R. 1997: Geochemistry of Tertiary tholeiites and picrites from Qeqertarsuaq (Disko Island) and Nuussuaq, West Greenland, with implications for mineral potential of comagmatic intrusions; *Contributions to Mineralogy and Petrology*, v. 128, p. 139–163.
- Macek, J.J. 1985a: Cat Creek; Manitoba Energy and Mines, Preliminary Map 1985C-1, scale 1:10 000.
- Macek, J.J. 1985b: Cat Creek project (parts of 52L/1, 8); *in Report of Activities 1985*, Manitoba Energy and Mines, Mineral Resources Division, p. 122–129.
- Mackie, R.A. 2003: Emplacement history and PGE-enriched sulphide mineralization of the heterolithic breccia zone in the Mayville intrusion; B.Sc. thesis, University of Manitoba, Winnipeg, Manitoba, 135 p.
- Maier, W., Barnes, S.J., Chinyepi, G., Barton, J.M., Eglington, B. and Setschedi, I. 2008: The composition of magmatic Ni-Cu-(PGE) sulfide deposits in the Tati and Selebi-Phikwe belts of eastern Botswana; *Mineralium Deposita*, v. 43, p. 37–60.
- Mantle, G.W. and Collins, W.J. 2008: Quantifying crustal thickness variations in evolving orogens: correlation between arc basalt composition and Moho depth; *Geology*, v. 36, p. 87–90.
- McDonough, W.F. and Sun, S.-s. 1995: The composition of the Earth; *Chemical Geology*, v. 120, p. 223–253.
- Mealin, C.A. 2008: Geology, geochemistry and Cr-Ni-Cu-PGE mineralization of the Bird River sill: evidence for a multiple intrusion model; MSc thesis, University of Waterloo, Waterloo, Ontario, 155 p.
- Metsaranta, R.T and Houlé, M.G., in press. Project Unit 10-004: McFaulds Lake area regional compilation and bedrock mapping project update; *in Summary of Field Work and Activities 2011*, Ontario Geological Survey, Open File Report 6270, p. 12-1–12-11.
- Mullen, E.D. 1983: MnO/TiO₂/P₂O₅; a minor element discriminant for basaltic rocks of oceanic environments and its implications for petrogenesis; *Earth and Planetary Science Letters*, v. 62, p. 53–62.
- Murphy, L.A. and Theyer P. 2005: Geology, structure and mineralization of the Ore Fault property, Bird River greenstone belt, southeastern Manitoba (parts of NTS 52L5NE and 52L6NW); *in Report of Activities 2005*, Manitoba Industry, Economic Development and Mines, Manitoba Geological Survey, p. 156–160.
- Mustang Minerals Corp. 2011: Annual Report 2010; Mustang Minerals Corp., 40 p.
- Pearce, J.A. 1983: Role of the sub-continental lithosphere in magma genesis at active continental margins; *in Continental Basalts and Mantle Xenoliths*, C.J. Hawkesworth and M.J. Norry (ed.), Shiva Publishing Limited, Nantwich, United Kingdom, p. 230–249.
- Pearce, J.A. 1996: A user's guide to basalt discrimination diagrams; *in Trace Element Geochemistry of Volcanic Rocks: Applications for Massive Sulphide Exploration*, D.A. Wyman (ed.), Geological Association of Canada, Short Course Notes 12, p. 79–113.

- Pearce, J.A. and Peate, D.W. 1995: Tectonic implications of the composition of volcanic arc magmas; *Annual Review of Earth and Planetary Sciences*, v. 23, p. 251–285.
- Peck, D.C., Keays, R.R., James, R.S., Chubb, P.T. and Reeves, S.J. 2001: Controls on the formation of contact-type platinum-group element mineralization in the East Bull Lake intrusion; *Economic Geology*, v. 96, p. 559–581.
- Peck, D.C., Scoates, R.F.J., Theyer, P., Desharnais, G., Hulbert, L.J. and Huminicki, M.A.E. 2002: Stratiform and contact-type PGE-Cu-Ni mineralization in the Fox River Sill and the Bird River Belt, Manitoba; in *The Geology, Geochemistry, Mineralogy and Mineral Beneficiation of Platinum-Group Elements*, L.J. Cabri (ed.), Canadian Institute of Mining and Metallurgy, Special Volume 54, p. 367–387.
- Peck, D.C., Theyer, P., Bailes, A.H. and Chornoboy, J. 1999: Field and lithogeochemical investigations of mafic and ultramafic rocks and associated Cu-Ni-PGE mineralization in the Bird River greenstone belt (parts of NTS 52L); in *Report of Activities, 1999*, Manitoba Industry, Trade and Mines, Geological Services, p. 106–110.
- Peck, D.C., Theyer, P., Hulbert, L., Xiong, J., Fedikow, M.A.F. and Cameron, H.D.M. 2000: Preliminary exploration database for platinum-group elements in Manitoba; Manitoba Industry, Trade and Mines, Manitoba Geological Survey, Open File OF2000-5, CD-ROM.
- Peltonen, P., Kontinen, A. and Huhma, H. 1998: Petrogenesis of the mantle sequence of the Jormua Ophiolite (Finland): melt migration in the upper mantle during Palaeoproterozoic continental break-up; *Journal of Petrology*, v. 39, p. 297–329.
- Percival, J.A. 2007: Geology and metallogeny of the Superior Province, Canada; in *Mineral Deposits of Canada: A Synthesis of Major Deposit-Types, District Metallogeny, the Evolution of Geological Provinces, and Exploration Methods*, W.D. Goodfellow (ed.), Geological Association of Canada, Mineral Deposits Division, Special Publication 5, p. 903–928.
- Percival, J.A., McNicoll, V. and Bailes, A.H. 2006a: Strike-slip juxtaposition of ca. 2.72 Ga juvenile arc and >2.98 Ga continent margin sequences, and its implications for Archean terrane accretion, western Superior Province, Canada; *Canadian Journal of Earth Sciences*, v. 43, p. 895–927.
- Percival, J.A., Sanborn-Barrie, M., Skulski, T., Stott, G.M., Helmstaedt, H. and White, D.J. 2006b: Tectonic evolution of the western Superior Province from NATMAP and LITHOPROBE studies; *Canadian Journal of Earth Sciences*, v. 43, p. 1085–1117.
- Plank, T. and Langmuir, C.H. 1988: An evaluation of the global variations in the major element chemistry of arc basalts; *Earth and Planetary Science Letters*, v. 90, p. 349–370.
- Rollinson, H.R. 1993: Using geochemical data: evaluation, presentation, interpretation; Longman Scientific & Technical, London, United Kingdom, 352 p.
- Schwartz, J.J., Johnson, K., Miranda, E.A. and Wooden, J.L. 2011: The generation of high Sr/Y plutons following Late Jurassic arc-arc collision, Blue Mountains province, NE Oregon; *Lithos*, v. 126, p. 22–41.
- Scoates, R.F.J. 1983: A preliminary stratigraphic examination of the ultramafic zone of the Bird River Sill, southeastern Manitoba; in *Report of Field Activities, Manitoba Department of Energy and Mines, Mineral Resources Division*, p. 70–83.
- Scoates, R.F.J., Williamson, B.L., Eckstrand, O.R. and Duke, J.M. 1989: Stratigraphy of the Bird River Sill and its chromitiferous zone, and preliminary geochemistry of the chromitite layers and PGE-bearing units, Chrome property, Manitoba; in *Investigations by the Geological Survey of Canada in Manitoba and Saskatchewan during the 1984–1989 Mineral Development Agreements*, A.G. Galley (ed.), Geological Survey of Canada, Open File 2133, p. 69–82.
- Stevenson, R.K., Berneir, F., Courteau, G. and Achado, N. 2000: Nd isotopic studies of the buried Precambrian crust in southern Manitoba; in *Western Superior Transect 6th Annual Workshop*, R.M. Harrap and H.H. Helmstaedt (ed.), LITHOPROBE Secretariat, University of British Columbia, Vancouver, BC, LITHOPROBE Report 77, p. 116–118.
- Sun, S.-s. and McDonough, W.F. 1989: Chemical and isotopic systematics of oceanic basalts: implications for mantle composition and processes; in *Magmatism in the Ocean Basins*, A.D. Saunders and M.J. Norry (ed.), Geological Society, Special Publication 42, p. 313–345.
- Syme, E.C. 1998: Ore-associated and barren rhyolites in the central Flin Flon belt: case study of the Flin Flon mine sequence; Manitoba Energy and Mines, Geological Services, Open File OF98-9, 26 p.
- Syme, E.C., Lucas, S.B., Bailes, A.H. and Stern, R.A. 1999: Contrasting arc and MORB-like assemblages in the Paleoproterozoic Flin Flon Belt, Manitoba, and the role of intra-arc extension in localizing volcanic-hosted massive sulphide deposits; *Canadian Journal of Earth Sciences*, v. 36, p. 1767–1788.
- Taylor, S.R. and McLennan S.M. 1985: The continental crust: its composition and evolution; Blackwell, Oxford, United Kingdom, 312 p.
- Tatsumi, Y. and Eggins, S. 1995: Subduction zone magmatism; Blackwell Science, Cambridge, Massachusetts, 211 p.
- Theyer, P. 1986: Platinum group elements in southeastern Manitoba; in *Report of Field Activities 1986*, Manitoba Energy and Mines, Geological Services Branch, p. 125–130.
- Theyer, P. 1991: Petrography, chemistry and distribution of platinum and palladium in ultramafic rocks of the Bird River Sill, SE Manitoba, Canada; *Mineralium Deposita*, v. 26, no. 3, p. 165–174.
- Theyer, P. 2003: Platinum group element investigations in the Mayville igneous complex, southeastern Manitoba (NTS 52L12); in *Report of Activities 2003*, Manitoba Industry, Trade and Mines, Manitoba Geological Survey, p. 196–199.
- Trueman, D.L. 1971: Petrological, structural and magnetic studies of a layered basic intrusion—Bird River Sill, Manitoba; M.Sc. thesis, University of Manitoba, Winnipeg, Manitoba, 67 p.

- Trueman, D.L. 1980: Stratigraphy, structure and metamorphic petrology of the Archean greenstone belt at Bird River, Manitoba; Ph.D. thesis, University of Manitoba, Winnipeg, Manitoba, 150 p.
- Trueman, D.L. and Turnock, A.C. 1982: Bird River greenstone belt, southeast Manitoba; geology and mineral deposits; Field Trip Guidebook, Geological Association of Canada–Mineralogical Association of Canada, Joint Annual Meeting, Winnipeg, Manitoba, Trip 9, p. 1–37.
- Wang, X. 1993: U-Pb zircon geochronology study of the Bird River greenstone belt, southeastern Manitoba; M.Sc. thesis, University of Windsor, Windsor, Ontario, 96 p.
- Watson, D.M. 1985: Chromite reserves of the Bird River Sill; Manitoba Energy and Mines, Geological Services, Open File OF85-8, 22 p.
- Williamson, B.L. 1990: Geology of the Bird River Sill at the Chrome property, southeast Manitoba; Geological Survey of Canada, Open File 2067, 44 p.
- Yang, X.M., Lentz, D.R., Chi, G. and Thorne, K.G. 2008: Geochemical characteristics of gold-related granitoids in southwestern New Brunswick, Canada; *Lithos*, v. 104, p. 355–377.
- Zhang, M., O'Reilly, S.Y., Wang, K.L., Hronsky, J., and Griffin, W.L. 2008: Flood basalts and metallogeny: the lithospheric mantle connection; *Earth-Science Reviews*, v. 86, p. 145–174.